

Glass-transition dynamics of a polyurethane gel using ultrasonic spectroscopy, dynamic light scattering, and dynamical mechanical thermal analysis

M. Tabellout, P.-Y. Baillif, H. Randrianantoandro, F. Litzinger, and J. R. Emery

Laboratoire d'Ultrasons, Physique de l'Etat Condensé URA CNRS, Université du Maine, 72017 Le Mans Cedex, France

T. Nicolai and D. Durand

Laboratoire de Physico-Chimie Macromoléculaire, URA CNRS, Université du Maine, 72017 Les Mans Cedex, France

(Received 16 June 1994)

The glass-transition dynamics of a polyurethane gel were studied over a wide temperature and frequency range using ultrasonic spectroscopy (US), dynamic light scattering (DLS), and dynamical mechanical thermal analysis (DMTA). DMTA showed both an α and a β relaxation, while with DLS only the α relaxation could be observed. The α relaxation measured by DLS and DMTA was analyzed in terms of a continuous relaxation time distribution. This analysis method is compared to an analysis in terms of the Kohlrausch-Williams-Watts function for the DLS results and the Havriliak-Negami function for the DMTA results. The shape of the relaxation time distribution is temperature independent over the temperature range covered and identical for both techniques. The temperature dependence of the characteristic relaxation rates is well described by the so-called Vogel-Fulcher-Tamman-Hesse equation. Characteristic relaxation rates measured by DLS were about a factor 10 smaller than interpolated from the US and DMTA measurements. Since DLS measures a compliance and the two other techniques a modulus, lower values are expected. If the compliance data are converted into corresponding values for the modulus, the DLS results are compatible with the US and DMTA results.

INTRODUCTION

The dynamics of the glass transition of polymeric systems have been studied by a large number of experimental techniques, e.g., nuclear magnetic resonance,¹ ultrasonic spectroscopy (US),²⁻⁴ Brillouin scattering (BS),^{5,6} dynamic light scattering (DLS),⁶⁻⁸ dielectric relaxation spectroscopy (DS),⁹ and dynamic mechanical techniques.¹⁰ Each technique has its own advantages and disadvantages in terms of, for instance, the accessible dynamical range and sample handling. In many ways the various techniques are complementary. It is therefore of particular interest to compare results of different techniques applied to the same system and to establish the extent to which the same dynamical processes are probed.

The glass-transition dynamics are generally characterized by at least two relaxational processes: the so-called α and β relaxations.^{11,12} The α relaxation is the local segmental relaxation of the polymer chain backbone, while the β relaxation is considered to be the side-group relaxation. Both relaxations are characterized by broad relaxation time distributions $A(\tau)$, the β relaxation being usually much broader than the α relaxation. Characteristic relaxation times (τ_c) can be defined in various ways, e.g., the average relaxation time, the position of the maximum in the relaxation time spectrum, or the parameter which characterizes the analytical function used to fit the data. If the functional form of $A(\tau)$ is known, τ_c values defined differently can of course be converted for comparison. The α relaxation is characterized by a strong non-Arrhenius temperature dependence, while the β relaxation has an Arrhenius temperature dependence

[$\log(\tau_c) \propto T^{-1}$]. At high temperatures the two processes merge and only a single relaxation is observed. When the two relaxations are distinct the α relaxation is much easier to measure and is better suited for a comparative study using different techniques. The temperature dependence of the characteristic relaxation rate of the α relaxation is found to be well described by the so-called Vogel-Fulcher-Tamman-Hesse (VFTH) equation:

$$\tau = \tau_0 \exp \left[\frac{B}{T - T_0} \right]. \quad (1)$$

Here τ_0 is the relaxation time in the high-temperature limit and T_0 is the temperature where τ becomes infinite. If this dynamical process is probed by techniques with different frequency ranges, the results can easily be compared by an appropriate choice of the measurement temperatures. In recent years comparative studies of the glass-transition dynamics have been done on a number of systems, mostly linear polymer liquids. Often the temperature dependence of the characteristic relaxation time is observed to be the same when probed by different techniques.¹³ The shape of the relaxation time distribution was found to be either independent of the temperature^{14,15} or to become narrower with increasing temperature.^{16,17} Even in the latter case the effect is only detectable if a large temperature range is scanned. As far as we are aware only one such study has been reported for a gel forming system.¹⁸

Here we present results of an investigation of the α relaxation of a polyurethane (PU) gel using a US, DLS, and DMTA. A comparison of these techniques is interesting

because the α relaxation is probed differently by each technique. In US the longitudinal modulus (M) is determined,¹⁹ while DLS is related to the longitudinal compliance (D),^{20,21} and in DMTA the Young's modulus²² (E) is measured. In addition the methods cover different complementing dynamical ranges. The results of DLS and DMTA were analyzed in terms of relaxation time distributions. The shape of the relaxation time distributions was found to be the same and independent of the temperature. The temperature dependence of the loss modulus peak position obtained from all three techniques can be described by the VFTH function with $B=1009$, $T_0=220$ K, and $\tau_0=8.3 \times 10^{-14}$ s. It will be shown that in order to determine the longitudinal modulus using US, it is necessary to measure both the ultrasonic absorption and the sound velocity at each frequency. Unfortunately, it was for the system studied here not possible to measure the sound velocity over a wide frequency range which is necessary for the determination of the shape of the relaxation function. In addition to the α relaxation a β relaxation with an Arrhenius temperature dependence was observed by DMTA.

EXPERIMENT

Materials. The polyurethane samples were formed by condensation of dried polyoxypropylene triol ($M_n=722$ g/mol, $M_w/M_n=1.03$) with hexamethylene diisocyanate (HMDI) in a stoichiometric ratio $r=[\text{NCO}]/[\text{OH}]$. The reaction was catalyzed by 2×10^{-3} g of dibutyltin dilaurate per gram of HMDI. The polycondensation was carried out at 313 K until complete consumption of the NCO groups. After two days, unreacted NCO groups could no longer be detected by IR spectroscopy. For light scattering measurements the initial mixture was filtered through Anotop filters with pore size $0.2 \mu\text{m}$ and the polycondensation occurred directly in the light scattering cells. The density of the polyurethane samples depends only weakly on r and is close to 1 g/ml at 293 K. The glass transition temperature T_g measured by differential scanning calorimetry (DSC) is 257 K for the polyurethane with stoichiometric ratio $r=1$.

DMTA. The DMTA measurements were done with a dynamical mechanical thermal analyzer from Polymer Laboratories. The samples were tested in a double cantilever bending with a fixed displacement ($\pm 16 \mu\text{m}$) in a temperature sweep mode. The sample temperature is controlled within 0.1 K in the range 123–323 K.

DLS. The DLS measurements were done on a Malvern K7032 or an ALV-5000 correlator in combination with a Malvern goniometer. The light source was an argon-ion laser emitting vertically polarized light with wavelength 488 nm. Depolarized DLS measurements were done by placing a Glan-Thompson polarizer before the photomultiplier. The temperature was controlled within 0.1 K using a thermostated bath. At low temperatures, water condensation was avoided by a constant nitrogen flow.

Assuming the validity of the Siegert relation, the experimental intensity autocorrelation functions [$G_2(t)$] are related to the normalized electric field autocorrelation

function [$g_1(t)$] in the following way:

$$\frac{G_2(t)}{\langle I \rangle^2} = g_2(t) = 1 + [bg_1(t)]^2, \quad (2)$$

where $\langle I \rangle$ is the time averaged scattered light intensity and b is a constant between 1 and 0 which depends on the experimental setup. For the setup used, b is approximately 0.6.

US. In US experiments, the measurements were made in transmission using a pulsed signal. To make measurements on very viscous samples, the transducers are maintained at a fixed distance in order to obtain the relative absorption and transit time variations with temperature. A spectroscopic method using fast Fourier transform^{23,24} (FFT) was used to determine the sound velocity (using FFT phase) and absorption (using FFT modulus) on a frequency domain limited by the transducer's bandwidth. The temperature was controlled within 0.1 K, using a thermostated bath. Transducers with fundamental frequency 7 MHz were used in this study.

RESULTS

DMTA. The Young's modulus was measured as a function of temperature between 123 and 323 K at a number of frequencies between 0.1 and 100 Hz. The loss modulus, E'' , shows two peaks: a relatively narrow peak at higher temperatures and a broader peak at lower temperatures, see Fig. 1. The narrow peak can be attributed to the α relaxation and the broad peak to the β relaxation. Characteristic frequencies can be obtained as a function of temperature either by taking the peak position in E'' vs T plots at different frequencies or in E'' vs frequency plots at different temperatures. The two methods give the same result. We have calculated the corresponding characteristic relaxation times using $\tau_c = (2\pi f_c)^{-1}$. E'' vs frequency plots have the same shape in the temperature range where we observe the α relaxation so that a master curve can be constructed by time-temperature superposition with $T_{\text{ref}}=260.4$ K, see

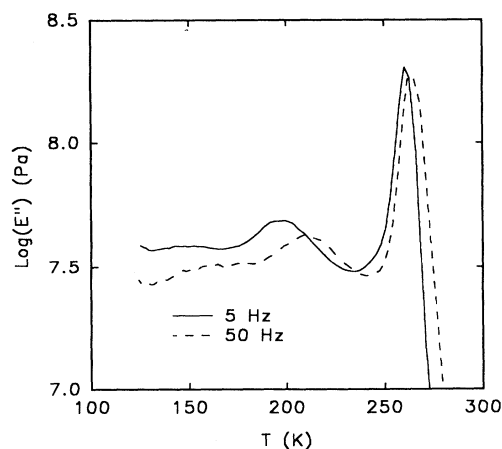


FIG. 1. Temperature dependence of the Young's loss modulus of the polyurethane gel (PU) with $r=1$ at two frequencies.

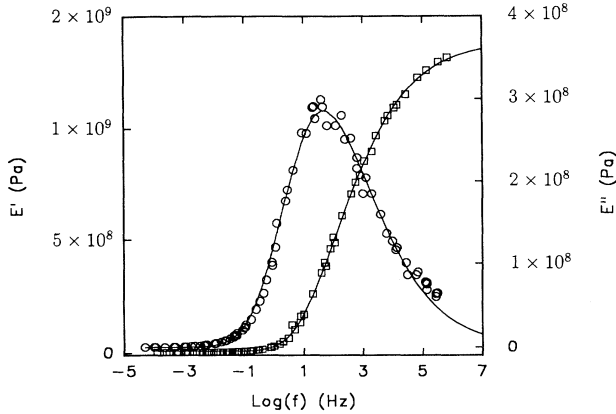


FIG. 2. Semilogarithmic master plots of the loss and storage Young's moduli for PU with $r=1$ versus frequency at reference temperature 260.4 K. The solid line represents the result of a fit to the GEX function [Eqs. (4) and (5)].

Fig. 2. Using the shift factors, the temperature range for which τ_c can be determined is much wider than when we restrict ourselves to the peak positions. Values of τ_c are shown in Fig. 3 in the form of an Arrhenius plot together with the results from DLS and US discussed below. In this representation the temperature dependence of τ_c characterizing the β relaxation is linear while the temperature dependence of the narrow mode shows a curvature typical for the α relaxation.

We have analyzed the data by assuming that the relaxation function characterizing the α relaxation [$\phi(t)$] is a continuous sum of exponentials:

$$\phi(t) = \int_0^\infty A(\tau) \exp(-t/\tau) d\tau. \quad (3)$$

The loss and storage modulus can now be written in terms of $A(\tau)$:

$$E''(\omega) = (E_\infty - E_0) \int_{-\infty}^\infty \frac{\omega\tau}{1 + \omega^2\tau^2} A(\tau) d\tau, \quad (4a)$$

$$E'(\omega) = E_0 + (E_\infty - E_0) \int_{-\infty}^\infty \frac{\omega^2\tau^2}{1 + \omega^2\tau^2} A(\tau) d\tau, \quad (4b)$$

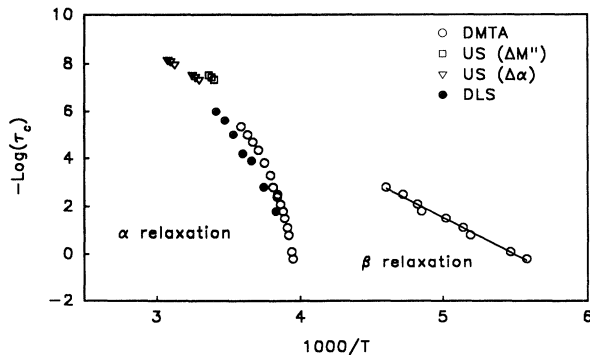


FIG. 3. Arrhenius plot of the temperature dependence of the characteristic relaxation times obtained from DLS, DMTA, and US measurements.

where E_∞ and E_0 are the high and low frequency limits, respectively, and $\omega = 2\pi f$ is the angular frequency. For $A(\tau)$ we have used the so-called generalized exponential (GEX) function:²⁵

$$A(\tau) = \frac{|s| \tau^{p-1} \tau_{\text{GEX}}^{-p} \exp(-\tau/\tau_{\text{GEX}})^s}{\Gamma(p/s)}, \quad (5)$$

where $\Gamma(x)$ is the gamma function. The GEX function has a large degree of freedom to describe single peaked distributions of widely different forms and has been used successfully to describe broad relaxation time distributions in DLS experiments.^{26,27} Two other functional forms are often used to describe the α relaxation: the Kohlrausch-Williams-Watts (KWW) function in the time domain:

$$\phi(t) = \exp[-(t/\tau_{\text{KWW}})^\beta] \quad (6)$$

and the Havriliak-Negami (HN) function in the frequency domain:

$$\phi^*(\omega) = \frac{1}{[1 + (i\omega\tau_{\text{HN}})^\alpha]^\gamma}. \quad (7)$$

The relation between these two latter functions is explored in Ref. 28. General properties of the GEX function and its relation to the HN and KWW functions are discussed elsewhere.³⁵ The main advantages of using the GEX function are that it can be used readily to analyze data in the frequency or the temperature domain and that a tractable expression for the relaxation distribution is obtained. The GEX function is therefore more suitable for a comparison of results from different techniques made on the time (DLS) and frequency (US and DMTA) domain. The GEX distribution gives a good representation of the experimental data except at very low frequencies, see the solid lines in Fig. 2. The values of the parameters obtained by a nonlinear least-squares fit to the E' data ($\tau_{\text{GEX}} = 7 \times 10^{-3}$ s, $p = 0.32$, $s = 0.33$, $E_0 = 9.6 \times 10^6$ Pa, $E_\infty = 1.4 \times 10^9$ Pa) were used to calculate the solid

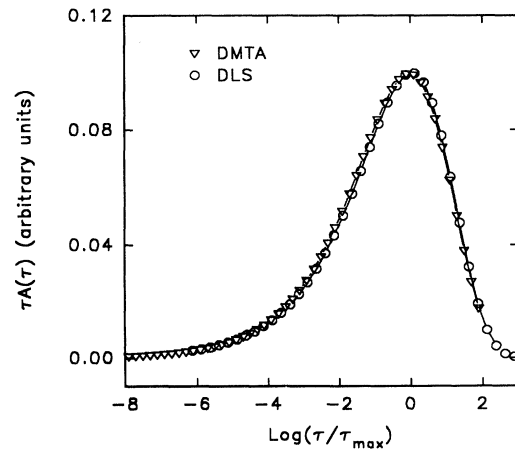


FIG. 4. Normalized relaxation time distribution functions characterizing the α relaxation obtained from a fit of the DLS and the DMTA measurement to Eq. (5).

line through the less well-defined E'' data. The corresponding relaxation time distribution is shown in Fig. 4 together with the results from DLS, see below. At very low frequencies, relaxations other than the α relaxation become apparent. These relaxations are due to dynamics of the polymer chains on larger distance scales and are called the Rouse normal modes. The large scale dynamics depend on the structure of the gel as is illustrated in Figs. 5(a) and 5(b) where E' and E'' are plotted for polyurethane gels prepared with different stoichiometric ratios as a function of f/f_c . In the double logarithmic representation, the onset of the Rouse modes is clearly visible at $f/f_c < 10^{-3}$ or possibly even at higher values of f/f_c . For comparison we also show the result of a fit to the HN function ($\tau_{\text{HN}}=0.1$ s, $\alpha=0.73$, $\gamma=0.27$). Using this function one can also fit the low frequency data since the data show a power-law dependence in the low frequency range. However, this behavior is due to the influence of Rouse normal modes, and the α relaxation is probably better described by a stretched exponential. The lower frequency relaxations are much better ex-

plored with other experimental techniques and will be discussed elsewhere.

Dynamic light scattering. Light scattering measurements on gels are often hampered by scattering from structural inhomogeneities.²⁹ For polyurethane gels this scattering is very strong and dominates the scattering from the density fluctuations. Interestingly, the depolarized scattering is almost as strong, implying high structural order. The restructuring is extremely slow and most of the scattering can be considered static on the time scale of the measurements (a few hours). The scattering from the inhomogeneities heterodynes the scattering from the density fluctuations resulting in reduced intercepts of the measured correlograms. The very low values of the intercepts mean that we can treat the correlation functions as fully heterodyne. In the heterodyne mode the intensity autocorrelation function is directly proportional to the electric field autocorrelation function.³⁰ In Fig. 6 the experimental correlation function at 293 K is shown. The fast relaxation which is independent of the scattering angle and has a strong temperature dependence can be identified with the α relaxation. This part of the correlation function can be related to the relaxation of the longitudinal compliance.^{20,21,31} At long times, the effect of structural relaxation can be detected. Fortunately, the relaxation times of the two modes remain well separated over the temperature range investigated (263–293 K) so that it is possible to cut off the correlograms before the second decay and treat the second decay as a floating baseline. When we subtract the baseline and normalize the intercepts, the correlograms measured at different temperatures have the same shape, but with a strongly temperature-dependent characteristic relaxation time, see Fig. 7(a). By doing a time-temperature shift, a master curve can be formed taking $T_{\text{ref}}=293$ K, see Fig. 7(b). The resulting master curve represents the relaxation function of the longitudinal compliance. We have analyzed the master curve again using Eqs. (3) and (5). The solid line through the data represents the result of a nonlinear least-squares fit ($\tau_{\text{GEX}}=1.5 \times 10^{-6}$ s, $p=0.32$, $s=0.34$). At long times,

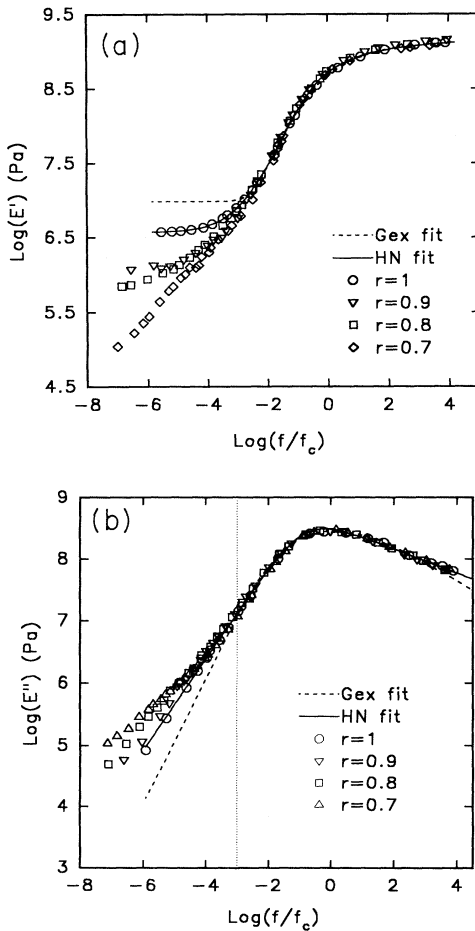


FIG. 5. (a) Double logarithmic master plots of the storage Young's modulus versus frequency for different stoichiometric ratios (r). The solid and dashed lines represent, respectively, results from a fit to the HN and the GEX function of the master plot at $r=1$. (b) The same as (a) for the Young's modulus.

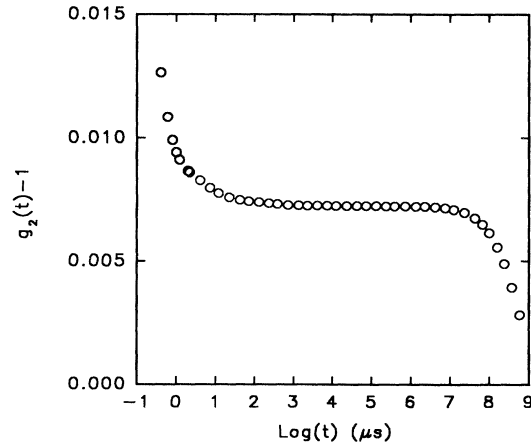


FIG. 6. Semilogarithmic plot of the intensity autocorrelation function of PU with $r=1$ measured at 293 K.

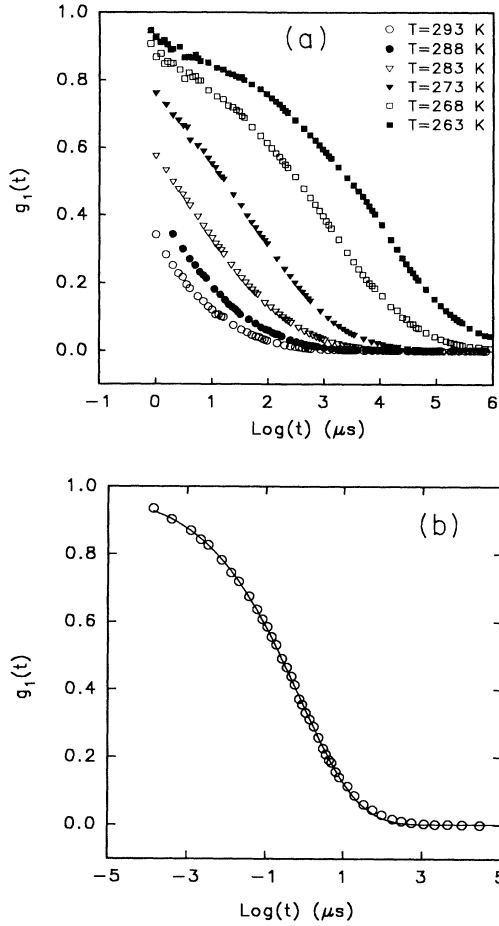


FIG. 7. (a) Normalized correlation functions after baseline subtraction at different temperatures of PU with $r=1$. (b) Master plot obtained by time-temperature superposition of the data shown in (a) with reference temperature 293 K. The solid line represents the result from a fit to the GEX function (Eqs. 3 and 5).

but before the onset of the structural relaxations, again an additional slow relaxation can be detected with a relatively small amplitude. The corresponding relaxation time distribution is shown in Fig. 4. The KWW function with $\beta=0.31$ and $\tau_{\text{KWW}}=0.74 \times 10^{-6}$ s describes the data almost as well except again at long times. Knowing $A(\tau)$, we can calculate the loss (D'') and storage (D') longitudinal compliance using

$$D''(\omega) = (D_0 - D_\infty) \int_{-\infty}^{\infty} \frac{\omega\tau}{1 + \omega^2\tau^2} A(\tau) d\tau \quad (8a)$$

and

$$D'(\omega) = D_\infty + (D_0 - D_\infty) \int_{-\infty}^{\infty} \frac{1}{1 + \omega^2\tau^2} A(\tau) d\tau, \quad (8b)$$

where $D_\infty = 1/M_\infty$ and $D_0 = 1/M_0$ are, respectively, the high and low frequency limits. Since we could not determine D_∞ and D_0 by DLS, we have calculated only relative values of D' and D'' , see Fig. 8. Taking again the maximum position of the loss peak as the characteristic frequency, we find $\tau_c = 1.0 \times 10^{-6}$ Hz at 293 K. Values

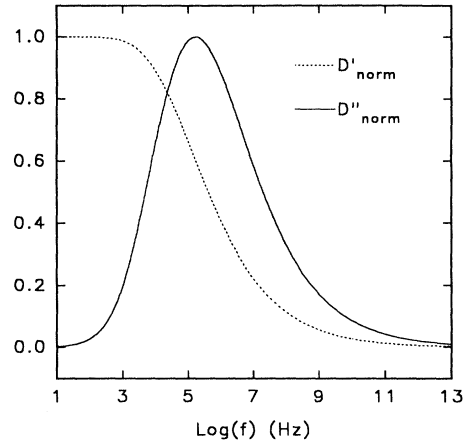


FIG. 8. Normalized loss and storage compliance of PU with $r=1$ obtained from DLS versus frequency at reference temperature 293 K.

of τ_c at other temperatures were calculated from the shift factors and are compared with DMTA and US results in Fig. 3.

Ultrasonic measurements. In US the measured experimental parameters are the sound velocity (v) and the ultrasonic absorption (α). For the sample studied here only the relative variation in the absorption ($\Delta\alpha$) could be measured. The temperature dependence of the v_L (longitudinal velocity) and $\Delta\alpha$ are shown for $f=4.5$ MHz in Fig. 9. The plot of $\Delta\alpha$ vs T shows a maximum due to the relaxation of density fluctuations. It is tempting to obtain f_c as a function of the temperature by taking the peak position plots of $\Delta\alpha$ vs T at different frequencies. However, values of f_c obtained in this way are not the same as the characteristic frequencies of the mechanical modulus since the longitudinal modulus (M) is a combination of the sound velocity and the ultrasonic absorption¹⁹

$$M'' = 2\rho v^3 \frac{\alpha}{\omega}, \quad (9a)$$

$$M' = \rho v^2, \quad (9b)$$

where ρ is the density. A plot of $\Delta M''$ vs T shows again a maximum but the peak position is shifted to lower temperature by 9 K, due to the dispersion of v , see Fig. 10. In the calculation of M'' we have neglected the very weak temperature variation of the density. It is clear that if we want to study the mechanical modulus at ultrasonic frequencies we have to measure both the temperature dependence of v and α as a function of the frequency. Unfortunately, for very viscous solutions, v can only be measured over a very limited range of low frequencies. In the past it has been assumed either that the dispersion of v can be neglected or that the values of v measured at low frequencies can be used to calculate M'' at higher frequencies.^{3,4} That these assumptions may lead to significant errors is evident from a comparison of Fig. 9 with Fig. 10. We are therefore limited to low frequency values. The peak positions are plotted in Fig. 3. For comparison we have also plotted the peak positions of $\Delta\alpha$

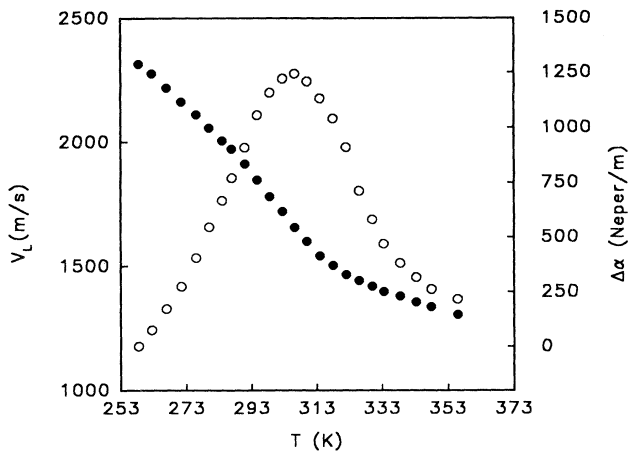


FIG. 9. Sound velocity and variation of the ultrasonic absorption of PU with $r = 1$ versus temperature at 4.5 MHz.

at different frequencies. We were not able to construct the frequency dependence of α or v as only the relative variations of α could be measured and v could only be measured in a very small frequency range. An alternative approach used in Ref. 32 consists in analyzing the temperature dependence directly by using the temperature dependence of the characteristic frequency. However, this procedure supposes both that the shape of the relaxation function is temperature independent and that the temperature dependence of f_c is known with high accuracy over a wide temperature range.

DISCUSSION

The dynamical processes measured by the three techniques used in this study are not probed in the same way. The DMTA technique probes the Young's modulus which is related to the bulk (K) and shear (G) modulus in the following way:^{10,22}

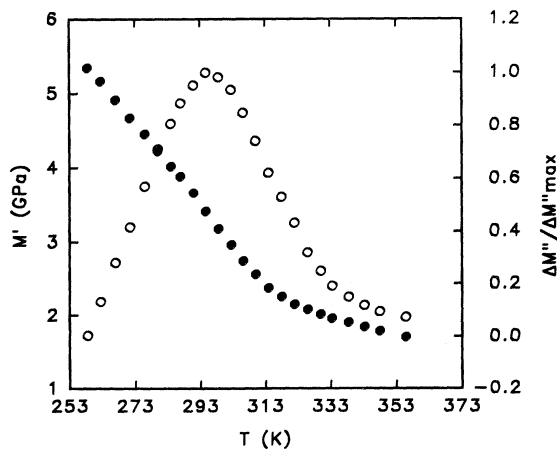


FIG. 10. Storage modulus and normalized variation of the loss modulus of PU with $r = 1$ obtained from US measurements versus temperature at 4.5 MHz.

$$E = \frac{9GK}{G + 3K} \quad (10)$$

In general, $K \gg G$ so that Eq. (10) reduces to $E = 3G$ which means with this technique one probes essentially the shear modulus. The longitudinal modulus measured by US is related to K and G as follows:³³

$$M = K + \frac{4}{3}G \quad (11)$$

Assuming again, $K \gg G$, Eq. (11) reduces to $M = K$ which implies that one measures essentially the bulk modulus. The fact that $M'/E' > 10$ for the polyurethane sample shows that we can indeed neglect the contribution of the bulk modulus to E and the contribution of the shear modulus to M . The electric field autocorrelation function due to density fluctuations is related to the relaxation function of the longitudinal compliance.^{20,21} Neglecting again the contribution of the shear compliance this means that by DLS the bulk compliance (B) is probed.

For a proper comparison of the DLS results with the DMTA and US results, we need to convert the compliance data to the corresponding modulus values using

$$M'' = \frac{D''}{D'^2 + D''^2} \quad (12a)$$

$$M' = \frac{D'}{D'^2 + D''^2} \quad (12b)$$

However, to calculate even the relative variation of M' and M'' , we need to know M_∞/M_0 . This is illustrated in Fig. 11 where we have plotted M''/M''_{\max} for different values of M_∞/M_0 . It is clear that the larger M_∞/M_0 , the broader is the loss modulus peak and the more the peak position is shifted to higher frequencies. From the limiting high and low temperature velocities, we can estimate that $M_\infty/M_0 = 1.8 \pm 0.2$ in the temperature range of the DLS measurements. Using this value, we can calculate the loss modulus peak, which is somewhat broader

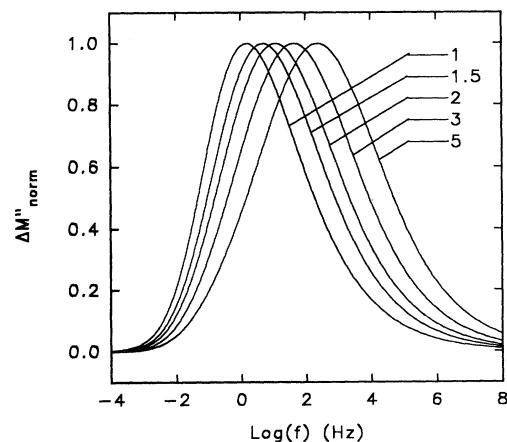


FIG. 11. Normalized loss moduli converted from the loss compliance data obtained from DLS for different values of M_∞/M_0 indicated in the figure.

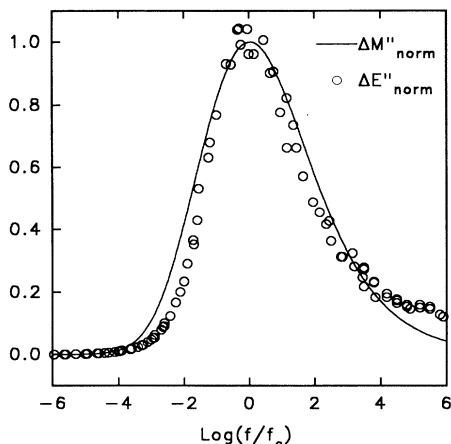


FIG. 12. Comparison of the normalized loss moduli obtained from DMTA and DLS.

than the DMTA results (see Fig. 12) and with the peak position at $f_c = 1.3 \times 10^6$ Hz. Using a similar procedure, Drake *et al.*²⁰ have compared the α relaxation of a simple liquid probed by DLS and US. They found a close agreement between the longitudinal moduli obtained by the two techniques.

We have plotted the characteristic relaxation times of the moduli obtained from US, DMTA, and DLS in the form of an Arrhenius plot, see Fig. 13. A nonlinear least-squares fit of the US and DMTA data to the VTFH equation yields $B = 1009$, $T_0 = 220$ K, and $\tau_0 = 8.3 \times 10^{-14}$ s. Given the uncertainty in the value of M_∞/M_0 , the results from DLS are compatible with the two other techniques. The fact that the loss peak obtained from DLS is slightly broader may be due to the larger influence of slow Rouse modes on the fit results. From mode-mode coupling theory,³⁴ a slightly narrower peak would be expected as the DLS measurements were done at higher temperatures. As is explained above, we were not able to measure the frequency dependence of the longitudinal modulus measured by US for the stoichiometry studied here. We are currently conducting a systematic investigation of the PU system at different stoichiometries. At stoichiometries below 0.6, the system does not gel so that the frequency dependence of M' can be measured and we can determine the relaxation time distribution. We expect that this study will enable us to establish whether the shape of the relaxation time distribution function has a significant temperature dependence.

In polymeric liquids there is a strong coupling between segmental rotation and translation in the glass-transition dynamics so that it is not surprising that the shear relaxation measured by DMTA is close to the longitudinal relaxation measured by the other techniques. The strong coupling is also indicated by the fact that, within experimental error, the same correlation function is measured in the polarized and depolarized modes.

Dynamic light scattering results are often analyzed in

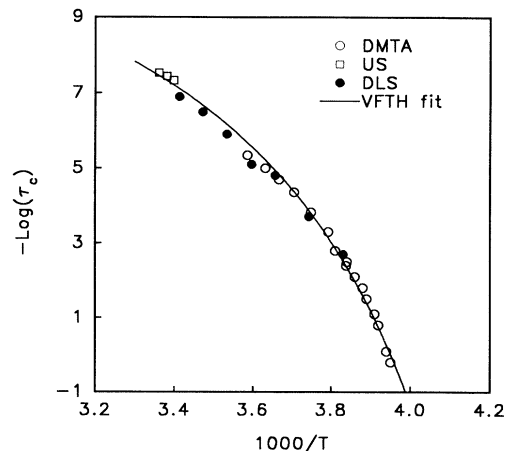


FIG. 13. Arrhenius plot of the temperature dependence of the characteristic relaxation times obtained from DLS (using converted data), DMTA, and US (obtained with M'' values) measurements. The solid line represents the result of a fit to the VTFH equation [Eq. (1)].

terms of the KWW function. For many polymeric liquids one obtains β values between 0.35 and 0.4. For the polyurethane gel we find a somewhat lower value (0.31) which might be due to the large structural polydispersity of the system.

CONCLUSIONS

The glass-transition dynamics in polyurethane gels are characterized by at least an α and a β relaxation. The dynamics of the α relaxation are close when measured using DMTA, DLS, and US, implying that the shear and bulk dynamics are similar. The temperature dependence of the α relaxation is well described by the VTFH equation: $\tau_c = 8.3 \times 10^{-14} \exp [1009/(T-220)]$. A continuous distribution of relaxation times, the so-called generalized exponential function, is well suited to analyze the α relaxation in both the DLS and the DMTA experiments. The relaxation distribution is independent of the temperature in the temperature range covered by DLS and DMTA and is somewhat broader than what is usually observed in polymeric liquids.

When the glass-transition dynamics are studied by US it is necessary to measure both the frequency dependence of the sound velocity and of the ultrasonic absorption. Contrary to what has been assumed in the literature, the dispersion of the sound velocity cannot be neglected. Only when both are known is it possible to calculate the frequency dependence of the longitudinal loss and storage moduli. A small contribution of slow relaxations probably due to Rouse normal modes can be detected by the DMTA and DLS measurements.

- ¹H. Sillescu, in *Polymer Motion in Dense System*, edited by D. Richter and T. Springer, Springer Proceedings in Physics, Vol. 29 (Springer-Verlag, Berlin, 1987).
- ²R. A. Pethrick, *Prog. Polym. Sci.* **9**, 197 (1983).
- ³I. Alig, F. Stieber, S. Wartewig, and G. Fytas, *Polymer* **29**, 975 (1988).
- ⁴I. Alig, F. Stieber, A. D. Bakhramov, Yu. S. Manucarov, and V. A. Solovyev, *Polymer* **30**, 842 (1989).
- ⁵G. D. Patterson, in *Dynamic Light Scattering, Applications of Photon Correlation Spectroscopy*, edited by R. Pecora (Plenum, New York, 1985), Chap. 6.
- ⁶G. Fytas and A. Patkowski, in *Dynamic Light Scattering, The Method and Some Applications*, edited by W. Brown (Clarendon, Oxford, 1993), Chap. 10.
- ⁷G. D. Patterson, *Adv. Polym. Sci.* **48**, 125 (1983).
- ⁸G. Fytas and G. Meier, in *Dynamic Light Scattering, The Method and Some Applications* (Ref. 6), Chap. 9.
- ⁹N. G. McCrum, B. E. Read, and G. Williams, *Anelastic and Dielectric Effects in Polymeric Solids* (Dover, New York, 1991).
- ¹⁰J. D. Ferry, *Viscoelastic Properties of Polymers*, 3rd ed. (Wiley, New York, 1980).
- ¹¹J. Perez, *Physique et Mécanique des Polymères Amorphes* (Tech. et Doc. Lavoisier, Paris, 1992).
- ¹²G. P. Johari, *The Glass Transition and the Nature of Glassy State* (The New York Academy of Science, New York, 1976).
- ¹³G. Floudas, G. Fytas, and E. W. Fischer, *Macromolecules* **24**, 1955 (1991); see also Refs. 14, 15, and 31.
- ¹⁴F. Kremer, D. Boese, G. Meier, and E. W. Fischer, *Progr. Coll. Polym. Sci.* **80**, 1 (1989).
- ¹⁵G. Fytas and K. L. Ngai, *Macromolecules* **21**, 804 (1988).
- ¹⁶R. W. Rendell, K. L. Ngai, and S. Mashimo, *J. Chem. Phys.* **87**, 2359 (1987).
- ¹⁷A. Dhinojwala, G. K. Wong, and J. M. Torkelson, *Macromolecules* **26**, 5943 (1993).
- ¹⁸I. Alig, D. Lellinger, K. Nancke, A. Rizos, and G. Fytas, *J. Appl. Polym. Sci.* **44**, 829 (1992).
- ¹⁹K. F. Herzfeld and T. A. Litovitz, *Absorption and Dispersion of Ultrasonic Waves* (Academic, New York, 1959).
- ²⁰P. W. Drake, J. F. Dill, C. J. Montrose, and R. Meister, *J. Chem. Phys.* **67**, 1969 (1977).
- ²¹C. H. Wang and E. W. Fischer, *J. Chem. Phys.* **82**, 632 (1985).
- ²²P. Gradin, P. G. Howgate, R. Seldén, and R. A. Brown, in *Comprehensive Polymer Science*, edited by C. Booth and C. Price (Pergamon, Oxford, 1989), Vol. 2, Chap. 16.
- ²³J. R. Emery and M. Tabellout, *Rev. Phys. Appl.* **25**, 243 (1990).
- ²⁴D. Lairez, D. Durand, and J. R. Emery, *Makromol. Chem., Macromol. Symp.* **45**, 31 (1991).
- ²⁵M. Kubin, *Collect. Czech. Commun.* **32**, 1505 (1967).
- ²⁶T. Nicolai, W. Brown, S. Hvidt, and K. Heller, *Macromolecules* **23**, 5088 (1990).
- ²⁷W. Brown and T. Nicolai, *Macromolecules* **27**, 2470 (1994).
- ²⁸F. Alvarez, A. Alegria, and J. Colmenero, *Phys. Rev. B* **44**, 7306 (1991).
- ²⁹E. Geissler, in *Dynamic Light Scattering, The Method and Some Applications* (Ref. 6), Chap. 11.
- ³⁰B. J. Berne and R. Pecora, *Dynamic Light Scattering* (Wiley, New York, 1976).
- ³¹G. Fytas, C. H. Wang, G. Meier, and E. W. Fischer, *Macromolecules* **18**, 1492 (1985).
- ³²G. Floudas, G. Fytas, and I. Alig, *Polymer* **32**, 2307 (1991).
- ³³G. Stokes, *Trans. Cambridge Philos. Soc.* **8**, 287 (1845).
- ³⁴C. M. Roland and K. L. Ngai, *Macromolecules* **24**, 5315 (1991).
- ³⁵T. Nicolai, J. C. Gimel, and R. Johnsen (unpublished).